Pergamon

0039-9140(94)00200-2

Talanta, Vol. 41, No. 12, pp. 2015–2023, 1994

0039-9140/94 $26.00 + 0.00

REVIEW

A SINGLE AND SIMPLE MATHEMATICAL EXPRESSION OF THE SIGNAL FOR CW-LASER THERMAL LENS SPECTROMETRY

J. GEORGES

Laboratoire des Sciences Analytiques, CNRS UA 435, Bât. 308, Université Claude Bernard-Lyon 1, 69622 Villeurbanne Cedex, France

(*Received* 25 *February* 1994. *Accepted* 24 *June* 1994)

Summary—Since the discovery of the thermal lens effect, several theoretical models have been put forward for cw-laser thermal lens spectrometry and different expressions of the thermal lens signal have been derived for various optical configurations including single-beam or dual-beam situations. This review focuses primarily on the successive mathematical expressions reported so far for both steady-state and time-resolved measurements, with the aim of comparing them in order to propose a single and convenient relation that accurately accounts for the sensitivity and the temporal behaviour of the thermal lens effect.

Thermal lens spectrometry is part of a class of highly sensitive absorbance methods based on the measurement of the temperature rise following the conversion of absorbed optical radiation into heat through non-radiative relaxation processes. These methods are generally classified into two categories: photoacoustic spectroscopy which refers to the generation of acoustic waves[1–3] and photothermal spectroscopy which detects a change in the refractive index of the solvent.[4–6] While photoacoustic spectroscopy is experiencing renewed interest owing to the greater optical power of lasers, photothermal methods are more recent and rely on the spatial coherence of laser radiation. These two classes of techniques are powerful tools complementary to other well known spectroscopic methods based on absorption and emission and are increasingly used by analysts for trace microchemical analysis[4,6–9] and by photochemists and biochemists to obtain energetic and kinetic information about transient species.[9–11]

In photothermal spectroscopy, the refractive index change generates an optical element within the sample, thus changing the propagation properties of a probe beam. Depending on the optical configuration and on the resulting optical element formed, several photothermal methods have been derived. The optical element is represented by a spherical lens in thermal lens spectrometry[12–15] and in colinear photothermal deflection,[16–19] a grating in photothermal diffraction[20] and a cylindrical lens in photothermal refraction.[21,22]

Laser-induced thermal lensing, which was discovered by Gordon *et al.*,[23] occurs as the result of light absorption by a Gaussian laser beam. Local heating near the beam axis produces a transverse temperature gradient which induces a refractive index gradient. The refractive index profile is approximately parabolic and behaves, for most liquids, as a negative lens which makes the laser beam to diverge. The thermal lens effect results in a spreading of the beam and a decrease in its intensity at the beam center. By measuring the far-field change in beam propagation, one can measure small absorbances and/or obtain information about the thermo-optical properties of the medium and the photophysical properties of the solute. Generally, the analytical signal is recovered by measuring the intensity variation at the center of a probe beam through a pinhole aperture with a photodiode. Less commonly, the thermal lens effect may be measured by recording the entire beam profile[24–26] with optical computation of spatial moments[27] or using Fourier analysis of the beam profile in the spatial frequency domain.[28,29] Although the beam profile method

is more accurate and less sensitive to spatial noise, the classical beam center measurement is more commonly used.

Since the first theoretical treatment of Gordon *et al.*,[23] various experimental configurations have been compared and several models have been derived for cw-laser thermal lens spectrometry, including single-beam and dual-beam configurations and steady-state as well as time-resolved measurements. The aim of this paper is to review and compare the successive models in order to correlate them and derive a single and simple mathematical expression of the thermal lens signal easily available for the users of the technique.

BASIS OF THE THERMAL LENS EFFECT

Consider a cw laser which operates in the TEM_{00} mode giving a Gaussian intensity distribution according to:

$$I(r) = \frac{2P}{\pi\omega^2}\exp\left(-\frac{2r^2}{\omega^2}\right), \quad (1)$$

where $I(r)$ and P are the input intensity at distance r from the axis and the total power of the laser beam, respectively, and ω is the beam radius defined as the distance r at which the field amplitude is 1/e the value on the axis.

If such a beam irradiates an absorbing sample, with incident intensity $I_0(r)$, the heat generated per unit length and unit time between r and $r + dr$ is given by:[23,30-32]

$$Q(r)\,dr = \frac{I_0(r)}{J}\alpha 2\pi r\,dr = \frac{2\alpha P}{J\pi\omega^2}\exp\left(-\frac{2r^2}{\omega^2}\right)2\pi r\,dr, \quad (2)$$

where $\alpha = \epsilon C$ is the absorption coefficient of the medium (cm^{-1}), ϵ is the decadic molar absorptivity ($l \cdot cm^{-1} \cdot mol^{-1}$) and C is the concentration of the analyte ($mol\,l^{-1}$). J, the Joule's coefficient, is 4.184 J/cal, if Q is expressed in $cal \cdot sec^{-1} \cdot cm^{-2}$ and P in J/sec or W.

Since the center ($r = 0$) of the laser beam is more intense than the edges, the heat generated results in the formation of a radial temperature distribution with maximum at $r = 0$:

$$\Delta T(r, t) = \frac{2\alpha P}{J\pi C_p \rho\omega^2}\int_0^t \left(\frac{1}{1 + 2t'/t_c}\right) \times \exp\left(-\frac{2r^2/\omega^2}{1 + 2t'/t_c}\right)dt', \quad (3)$$

where $t_c = \omega^2/4D = \omega^2\rho C_p/4k$ is a characteristic time constant, ρ, D, C_p and k are the density (g/cm^3), the thermal diffusivity (cm^2/sec), the specific heat ($cal \cdot g^{-1} \cdot K^{-1}$) and the thermal conductivity ($cal \cdot sec^{-1} \cdot cm^{-1} \cdot K^{-1}$), respectively. If it is preferred to express energy in Joule, then $J = 1$ and C_p and k are expressed in $J \cdot g^{-1} \cdot K^{-1}$ and $J \cdot sec^{-1} \cdot cm^{-1} \cdot K^{-1}$, respectively.

The variation of the refractive index with distance r and time is proportional to ΔT and is approximately given by:[23]

$$n(r, t) = n_0 + \frac{dn}{dT}\Delta T(r, t), \quad (4)$$

where n_0 is the refractive index at the initial temperature, and dn/dT (K^{-1}) is the refractive index gradient. For most liquids, an increase in T produces a decrease of the refractive index such that the actual optical path at the beam center is shorter than that in the edges. The resulting refractive index gradient creates a lens-like optical element which has an effect on the beam propagation beyond the sample cell.

The theory described in this review is based on a two-dimensional temperature model and involves several assumptions:

—the laser beam is Gaussian

—the sample is considered as an infinite medium with respect to the size of the beam and the spot size remains constant over the length of the sample cell

—the sample is homogeneous and is weakly absorbing so that the refractive index gradient dn/dT is constant and the beam profile is not changed within the sample

—thermal conduction is the main mechanism of heat transfer and only radial heat flow is considered.

Two cases will be considered depending on whether the experimental set-up involves a single-beam or a dual-beam arrangement. Although the dual-beam configuration is generally used, the optical simplicity of the single-beam configuration is sometimes preferred, especially when using the thermal lens method for detection in liquid chromatography.[33]

THE SINGLE-BEAM METHOD

The parabolic model[23,30,32]

The first model was based on a single laser beam which performs both functions of forming the lens in the sample and probing its presence.

The laser beam is treated as a line source, with the above assumptions, and the temperature gradient in the sample is given in terms of exponential integrals:

$$\Delta T(r,t)=\frac{\alpha P}{4\pi k}\times\left[Ei\left(-\frac{2r^2}{\omega^2}\right)-Ei\left(-\frac{1}{1+2t/t_c}\times\frac{2r^2}{\omega^2}\right)\right]. \quad (5)$$

(Now, J, taken as unity, is systematically omitted and the other variables are expressed in Joules as mentioned above.)

This expression cannot be solved without approximation. For temperatures near the axis, the curves for ΔT *vs.* the distance r, according to equation (5), are parabolic and the gradient may be approximated by expanding the exponential integrals in a power series, to terms in r:[2,23]

$$\Delta T(r,t)=\frac{\alpha P}{4\pi k}\left[\ln\left(1+\frac{2t}{t_c}\right)-\frac{2(r^2/\omega^2)}{1+t_c/2t}\right]. \quad (6)$$

The curves are in good agreement with this quadratic approximation in the vicinity of the beam axis, typically up to $r=\omega$.

Using the last expression of ΔT in equation (4), one obtains:

$$n(r,t)\approx n_0+\frac{dn}{dT}\frac{\alpha P}{4\pi k}\times\left[\ln\left(1+\frac{2t}{t_c}\right)-\frac{2(r^2/\omega^2)}{1+(t_c/2t)}\right]. \quad (7)$$

Since dn/dT is small, the r-independent term in the brackets contributes only a small part to the refractive index and can be dropped; the remaining quadratic expression is then written as:

$$n(r,t)\approx n_0[1+\delta(r/\omega)^2], \quad (8)$$

where:

$$\delta=-2\frac{dn}{dT}\frac{\alpha P}{4\pi k n_0[1+(t_c/2t)]}. \quad (9)$$

If the optical pathlength, l, is short, the parabolic radial refractive-index gradient, over the length l, acts as an ideal thin lens with focal length given by:

$$f(t)=-\frac{\omega^2}{2\delta l n_0} \quad (10)$$

$$f(t)=\frac{\pi k\omega^2}{\alpha l P(dn/dT)}\left[1+\frac{t_c}{2t}\right]. \quad (11)$$

The thermal lens is a time-dependent optical element and requires a finite time to develop within the sample. When $t\gg t_c$, a steady-state is reached meaning that the rate of heating equals the rate of heat loss out of the irradiation volume. The steady-state focal length can thus be expressed as:

$$f(\infty)=\frac{\pi k\omega^2}{2.3AP(dn/dT)}, \quad (12)$$

where A is the decadic absorbance. In this expression, it is assumed that all the absorbed energy ($2.3AP$) is converted to heat. Otherwise, a correction factor must be applied.

Based on this model, Hu and Whinnery[30] derived an expression which describes the variations in spot size and beam center intensity in the far field with respect to the absorbance of the sample and thermo-optical properties of the medium.

The experimental arrangement for single-beam thermal lens measurements is shown in Fig. 1. A converging lens focuses the laser beam to a minimum radius ω_0, or beam waist, taken as the origin of the optical system. The sample cell is placed at a distance Z_1 beyond this waist, and the expansion of the beam is measured at a distance Z_2 from the cell.[13,32] Using the ray transfer matrix method[13,14,32] yields the following expression for the far-field spot size at the steady-state:

$$\omega_2^2=\omega_0^2\left[\left(1-\frac{Z_2}{f(\infty)}\right)^2+\left(Z_1-\frac{Z_1Z_2}{f(\infty)}+Z_2\right)^2\Big/Z_c^2\right), \quad (13)$$

where $Z_c=\pi\omega_0^2/\lambda$ is the confocal distance. The sample pathlength must be small with respect to the confocal distance allowing the beam radius to be constant within the cell.

The effect of the thermal lens on the spot size maximizes in the far field when $Z_2\gg Z_c$; then the expression for the far-field spot size is simplified as:

$$\omega_2^2=\omega_0^2Z_2^2\left[\left(\frac{1}{f(\infty)}\right)^2+\left(1-\frac{Z_1}{f(\infty)}\right)^2\Big/Z_c^2\right]. \quad (14)$$

Finally, the signal is measured as the relative change in beam center intensity ($r=0$), sampled with a pinhole and expressed as $I_{bc}=2P/\pi\omega_2^2$, before [$t=0$, then $f(0)=\infty$] and after the formation of the thermal lens:

$$\frac{\Delta I_{bc}}{I_{bc}}=\frac{I_{bc}(0)-I_{bc}(\infty)}{I_{bc}(\infty)}=\frac{\omega_2^2(\infty)-\omega_2^2(0)}{\omega_2^2(0)} \quad (15)$$

$$\frac{\Delta I}{I}=-\frac{2Z_1}{f(\infty)}+\frac{Z_1^2+Z_c^2}{(f(\infty))^2}. \quad (16)$$

Considering that the thermal lens effect is weak, the quadratic term is neglected, and equation (16) becomes:

$$\frac{\Delta I}{I} = -\frac{2Z_1}{f(\infty)}. \tag{17}$$

Taking the expression for $f(\infty)$ and recalling that the beam spot size into the sample, ω_1, is defined as:

$$\omega_1^2 = \omega_0^2\left[\frac{Z_1^2 + Z_c^2}{Z_c^2}\right], \tag{18}$$

the dependence of the thermal lens signal on sample position along the beam axis is given by:

$$\frac{\Delta I}{I} = -\frac{2.3AP}{\lambda k}\left(\frac{dn}{dT}\right)\left[\frac{2Z_1 Z_c}{Z_1^2 + Z_c^2}\right]. \tag{19}$$

The effect of the thermal lens on the beam size in the far field depends on the size and the radius of curvature of the wavefronts for the beam at the sample position. Theoretically, for a weak thermal lens, the beam expands the most when the thermal lens is located at one confocal distance beyond the waist, $Z_1 = Z_c$, where $\omega = \sqrt{2}\omega_0$.[13,14,30]

Under these conditions, the expression for the thermal lens signal is reduced to:

$$\frac{\Delta I}{I} = \theta \tag{20}$$

where θ is a dimensionless parameter which indicates the strength of the thermal lens effect and depends on the sample absorbance, the laser power and the thermo-optical properties of the medium:

$$\theta = -\frac{2.3AP}{\lambda k}\left(\frac{dn}{dT}\right). \tag{21}$$

The aberrant thermal lens model[34,35]

The parabolic model has provided a good basis for understanding the behavior of the thermal lens, but has required a few corrections in order to achieve more accurate quantitative predictions. The refractive-index gradient is not parabolic out of the excitation beam and the thermal lens cannot be considered as an ideal thin lens.

Using Fresnel diffraction theory, Sheldon *et al.*[34] derived a more accurate expression of the thermal lens signal. This model incorporates the aberrant nature of the thermal lens which originates from deviations in the temperature profile with respect to an ideal parabolic distribution. Instead of approximating the exponential integrals with a power series as in the parabolic model, the expression for the temperature distribution is kept in integral form and the refractive index *vs.* radius and time is obtained by using ΔT of equation (3) in (4). The effect of the refractive-index gradient on beam propagation beyond the sample is then determined by using the diffraction theory of aberrations. Evaluation of the diffraction integral leads to an

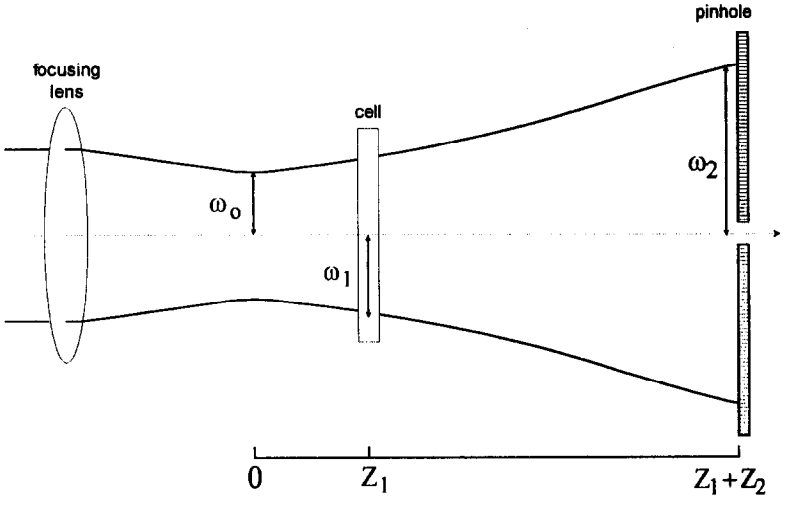

Fig. 1. Optical system for single-beam thermal lens measurements. The origin of the system is at the beam waist, ω_0, formed by a focusing lens. The sample cell is placed at a distance Z_1 beyond the waist, where the beam size is ω_1. The thermal lens effect is detected at a distance Z_2 from the cell and is measured as a change in the beam intensity.

expression for the relative intensity change at the beam center in the far field and at the steady-state:

$$\frac{\Delta I}{I} = -1 + \left[1 - \theta \tan^{-1}\left(\frac{2\gamma}{3+\gamma^2}\right)\right]^{-1} \quad (22)$$

instead of:

$$\frac{\Delta I}{I} = \theta\left(\frac{2\gamma}{1+\gamma^2}\right) \quad (23)$$

for the parabolic model, with $\gamma = Z_1/Z_c$. The sample position dependence, term in brackets in equation (22), predicts that the thermal lens signal is maximum when $Z_1 = \sqrt{3}Z_c$, *i.e.* when the cell is located at $\sqrt{3}$ the confocal distance beyond the waist. In this instance, the term

$$\tan^{-1}\left(2\gamma/(3+\gamma^2)\right) \text{ becomes } \tan^{-1}(0.577) = 0.52,$$

and the optimum thermal lens signal may be expressed as:[35]

$$\frac{\Delta I}{I} = -1 + [1 - 0.52\theta]^{-1}. \quad (24)$$

Using the series approximation,

$$(1+x)^{-1} = 1 - x + x^2 + \cdots,$$

and neglecting the term in θ^2, one obtains the final expression:

$$\frac{\Delta I}{I} = 0.52\theta. \quad (25)$$

This relation is quite similar to that obtained with the parabolic model, but both models disagree on the position of the sample cell for maximum signal and on the relative magnitude of the thermal lens signal. For a given value of θ, the parabolic model predicts an intensity change that is almost twice greater.

THE DUAL-BEAM METHOD

Both models previously described considered a single-laser configuration in which the thermal lens is generated and probed by the same beam. Later experimental developments involved a dual-beam configuration in which the thermal lens is created by a modulated cw-laser and probed by a second much weaker and very stable laser.[36] The pump-and-probe method allows the use of synchronous detection (lock-in amplifier) to detect the modulation on the probe beam center intensity by the thermal lens, which generally improves the signal-to-noise ratio over that obtained with the single-beam configuration. Moreover, the dual-beam configuration is necessary for recording absorption spectra, or when using pulsed-laser excitation.

Two kinds of dual-beam experimental arrangements, called mode-matched and mode-mismatched dual-beam thermal lens, have been developed.

The mode-matched configuration

In this arrangement, both beams are focused by the same lens and are assumed to propogate coincidently with distance. The radii of the pump and probe laser beams are matched at the sample position. The single-beam theory applies equally well, but should include a small correction for wavelength difference between the two beams:[37]

$$\frac{\Delta I}{I} = -\frac{2.3A_eP_e}{\lambda_p k}\left(\frac{dn}{dT}\right)_p, \quad (26)$$

where P_e is the power of the excitation laser, A_e is the absorbance of the sample at the excitation wavelength, λ_p is the wavelength of the probe laser and $(dn/dT)_p$ is the change in refractive index with temperature at the wavelength of the probe beam. If one defines a value of θ with respect to the wavelength of both beams, and taking into account the aberrant nature of the thermal lens, one may write:

$$\frac{\Delta I}{I} = 0.52\theta_{ep}. \quad (27)$$

However, in this arrangement, maximum signal results from a compromise: the effect of the thermal lens on the propogation of the probe beam is maximum around the confocal point of the probe laser while, at this position, the strength of the thermal lens is lower than that at the waist of the excitation beam.

The mode-mismatched configuration

Enhanced sensitivity is expected when the sample is positioned at the waist of the excitation laser and near the confocal position of the probe beam.[12,38] Such an arrangement is achieved by focusing the pump and probe beams by two separate lenses placed ahead of a beam splitter used to recombine the two beams.[25] Since the size of the excitation beam, ω_{e1}, at one confocal distance beyond its waist is $\omega_{e1} = \sqrt{2}\omega_{e0}$ (equation 18), the strength of the lens formed at the waist is twice stronger than that created at one confocal distance (equation 12).

However, additional considerations include the relative size of the two beams, as studied first

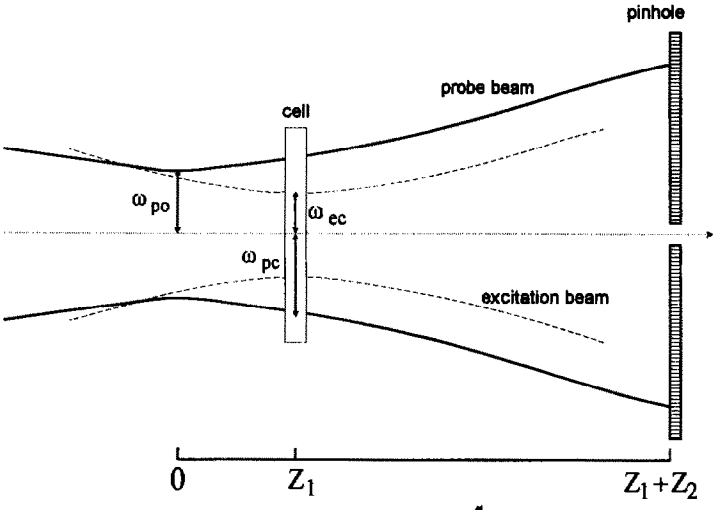

Fig. 2. Scheme of the optical system for mode-mismatched dual-beam thermal lens experiment. The cell is positioned at the waist of the excitation beam, $\omega_{ec} = \omega_{e0}$, and at a distance Z_1 from the waist of the probe beam, ω_{p0}, which is taken as the origin of the optical system along the beam axis.

by Berthoud *et al.*[39], assuming an ideal parabolic refractive index gradient, and then by Snook *et al.*,[40] taking the aberrant nature of the thermal lens into account.

The parabolic lens model. Berthoud *et al.* described the first theoretical model for mode-mismatched dual-beam thermal lens spectrometry which accounts for the relative beam size in the sample cell. Since the sample cell is positioned at the waist of the excitation beam and near the confocal point of the probe beam, the probe beam into the sample is generally much larger than the excitation beam, and only the central part of the probe beam is affected by the thermal lens (Fig. 2). Therefore, the intensity change of the probe beam at the detector is expressed on the basis of Gaussian beam diffraction theory: the probe beam at the detector contains two components, one component modified by the thermal lens and the other one independent of the thermal effect.

Keeping the same expression as in equation (15) for the steady-state thermal lens signal, and assuming that the variation of the beam size at the detector, $\Delta\omega_2$, is small with respect to ω_2, $\Delta I/I$ is expressed by the same relation corrected by the beam size ratio:[39]

$$\frac{\Delta I}{I} = 2\frac{\omega_{ec}^2}{\omega_{pc}^2}\left(\frac{\omega_2^2(\infty)}{\omega_2^2(0)} - 1\right), \qquad (28)$$

where ω_{ec} and ω_{pc} are the beam sizes into the sample cell of the excitation and probe beams, respectively, and $\omega_2^2(0)$ and $\omega_2^2(\infty)$ are the probe beam size at the detector before the formation of the thermal lens and at the steady-state, respectively.

Following the same calculation as for equation (17), one obtains:

$$\frac{\Delta I}{I} = -2\frac{\omega_{ec}^2}{\omega_{pc}^2}\left(\frac{2Z_1}{f(\infty)}\right), \qquad (28)$$

where $\omega_{ec} = \omega_{e0}$ is the waist of the excitation beam.

Using equations (12) and (21), $-1/f(\infty)$ may be expressed as $\theta\lambda_p/\pi\omega_{ec}^2$, and using equation (18) to express ω_{pc} with respect to its waist ω_{p0}, equation (28) becomes:

$$\frac{\Delta I}{I} = \frac{2\theta\lambda_p}{\pi\omega_{p0}^2}\left[\frac{2Z_1 Z_c^2}{Z_1^2 + Z_c^2}\right], \qquad (29)$$

where λ_p is the wavelength of the probe laser, and $Z_c = \pi\omega_{p0}^2/\lambda_p$ is the confocal distance of the probe laser. The position-dependent term in brackets in equation (29) maximizes for $Z_1 = Z_c$, leading to:

$$\frac{\Delta I}{I} = 4\frac{\omega_{p0}^2}{\omega_{pc}^2}\theta. \qquad (30)$$

Since for $Z_1 = Z_c$, $\omega_{pc} = \sqrt{2}\omega_{p0}$, equation (30) becomes finally:

$$\frac{\Delta I}{I} = 2\theta. \qquad (31)$$

Although this expression was derived from the parabolic model, maximum sensitivity was experimentally obtained when the cell was positioned at the waist of the excitation beam and at $Z_1 = \sqrt{3}Z_c$, as suggested by Fang and

Swofford[12] and then demonstrated in the aberrant model of Sheldon.[34] Therefore, the sensitivity expected from equation (31) is somewhat over-estimated. Assuming that the same correction as for a single-beam arrangement can be applied to take the aberrant nature of the lens into account, one obtains: $\Delta I/I \approx \theta$.

The aberrant lens model. More recently, Snook *et al.*[40] introduced a new theoretical model for cw-laser thermal lens spectrometry which is suitable for single-beam and dual-beam experiments. As in the Sheldon's model, the expression for the temperature gradient is kept as integral forms and the refractive index gradient into the sample is analysed as its effect on a phase shift of the probe beam. The probe beam is then treated with Fresnel diffraction theory using the complex amplitude of the electric field and considering only the central part of the probe beam at the detector plane. In this model, the steady-state thermal lens signal is best defined by:

$$\frac{\Delta I}{I} = \frac{I(\infty) - I(0)}{I(0)} \tag{32}$$

and finally expressed as:

$$\frac{\Delta I}{I} = \left[1 - \frac{\theta}{2}\tan^{-1}\left(\frac{2mV}{1+2m+V^2}\right)\right]^2 - 1, \tag{33}$$

where $V \approx Z_1/Z_c$, and $m = (\omega_{pc}/\omega_{ec})^2$, where ω_{pc} and ω_{ec} are the size, into the sample cell, of the probe and excitation beams, respectively. The beam size ratio, m, represents the degree of mode-mismatching of the probe beam and excitation beam. As seen from equation (33), the larger $\tan^{-1}[2mV/(1+2m+V^2)]$ is, the bigger is the signal, which means that the sensitivity of the thermal lens method increases when the degree of mode-mismatching increases.

The signal expression defined in equation (33) is general and applies equally well for all optical configurations. In single-beam experiments as well as in the mode-matched dual-beam configuration, $m = 1$ and the term $\tan^{-1}[2mV/(1+2m+V^2)]$ is the same as in the Sheldon's model and maximizes at 0.52 for $V = \sqrt{3}$, that is $Z_1 = \sqrt{3}Z_c$; in this instance, equation (33) becomes:

$$\frac{\Delta I}{I} = [1 - 0.26\theta]^2 - 1. \tag{34}$$

Since θ is small (for example: in water, with $A = 4 \times 10^{-3}$ and $P = 100$ mW, $\theta \cong 0.2$), equation (34) simplifies to the same relation as that derived by Sheldon:

$$\frac{\Delta I}{I} \approx -0.52\theta. \tag{35}$$

In the mode-mismatched dual-beam configuration, the optimum cell position (value of Z_1) is not precisely defined by equation (33). However, taking $Z_1 = \sqrt{3}Z_c$, *i.e.* $V = \sqrt{3}$, the plot of the steady-state signal $\Delta I/I$ *vs.* m fits to equation (33) and shows that maximum sensitivity is obtained when m is in the order of 30–40, *i.e.* when the size of the probe beam in the cell is about six to seven times greater than the size of the excitation beam.[40] Then, $\tan^{-1}[2mV/1+2m+V^2]$ maximizes at 1.0 and the amplitude of the thermal lens signal, equation (33), is given by the following simplified relation:

$$\frac{\Delta I}{I} = \left[1 - \frac{\theta}{2}\right]^2 - 1, \tag{36}$$

that is, for small values of θ:

$$\frac{\Delta I}{I} = -\theta. \tag{37}$$

[The minus in equations (35) and (37) comes from the fact that, in equation (32), the fractional intensity change is negative.]

In conclusion, the different models lead to similar results. When using a dual-beam mode-mismatched configuration, the steady-state thermal lens signal, with optimum adjusting of the sample position and beam size ratio, is well described by the following relation:

$$\frac{\Delta I}{I} = \pm\frac{2.3AP}{\lambda k}\left(\frac{dn}{dT}\right). \tag{38}$$

In the other cases, single-beam or mode-matched dual-beam configurations, the signal is almost twice smaller.

TIME-RESOLVED MEASUREMENTS

The build-up of the thermal lens signal under cw-laser excitation depends on the characteristic time constant $t_c = \omega^2\rho C_p/4k$.[41] The time-dependence of the signal is obtained by using a shutter to block or unblock the laser beam. The experiment begins when the shutter opens and is completed when the thermal lens is fully developed and the signal has reached a steady-state. When the characteristic time constant t_c is small, a chopper can be used, at a low frequency in order to let the thermal lens to relax completely between two chopper cycles. From the time-dependence of the signal, experimental values of t_c can be obtained leading to quantitative

information about the thermo-optical properties of the medium, such as thermal diffusivity, heat capacity or thermal conductivity.

As in the experiment of Gupta *et al.*,[42] carried out with pulsed-laser excitation, the method needs to use a reference solvent with known thermo-optical properties. However, the first experiments made on the basis of the parabolic model were not accurate[43] and steady-state measurements were most often used.

Two models taking the aberrant nature of the lens into account have been derived so far. In the first model developed for single-beam experiments, the predicted time-dependence of the thermal lens signal when the cell is located at $Z_1 = \sqrt{3}Z_c$ is written as:[34]

$$I(t) = I(0)\left[1 - \theta \tan^{-1}\frac{0.577}{(1 + t_c/t)}\right]. \quad (39)$$

More recently, a general equation that describes accurately the behaviour of the thermal lens signal has been developed by Snook *et al.*:[40]

$$I(t) = I(0)\left[1 - \frac{\theta}{2}\tan^{-1} \times\left(\frac{2mV}{[(1+2m)^2 + V^2](t_c/2t)+1+2m+V^2}\right)\right]^2. \quad (40)$$

Experimental data have been shown to fit to equation (40) for a wide range of the degree of mode-mismatching, m.[40] When $m = 1$, that is for single-beam or mode-matched dual-beam experiments, and taking $V = \sqrt{3}$, equation (40) becomes:

$$I(t) = I(0)\left[1 - \frac{\theta}{2}\tan^{-1}\left(\frac{0.577}{1 + t_c/t}\right)\right]^2 \quad (41)$$

which approximates to equation (39) of Sheldon.

The time-dependence of the thermal lens signal defined by equation (39)–(41) is compared in Fig. 3. For single-beam and mode-matched dual-beam configurations, both models agree quite well as shown by the fit of equations (39) and (40). For the mode-mismatched dual-beam method, the amplitude of the time-dependence is greater as expected from the steady-state signal expression. However, the time required to reach the steady-state is longer and increases when m increases. While the steady-state is reached for $t < 20t_c$ in single-beam and mode-matched dual-beam experiments, maximum sensitivity is obtained for longer times when using a high degree of mode-mismatching, typically $t > 100t_c$ when $m = 50$. This can be a drawback in experiments where it is required to work with a modulated excitation beam at a frequency high enough, *i.e.* 20–40 Hz, in order to improve the signal-to-noise ratio and the peak resolution for the detection of flowing samples, such as in flow injection analysis or in liquid chromatography. In this instance, it is no longer advantageous to work with a high degree of mode-mismatching because the steady-state is not reached during a chopper cycle and maximum sensitivity cannot be achieved. The best compromise seems to be obtained with a low degree of mode-mismatching ($m \cong 4$, that is a probe beam twice greater than the excitation beam), allowing both a fast thermal lens equilibrium and a better sensitivity.

The accuracy of theoretical equations with experimental results[40] indicates the possibility for the absolute measurement of weak absorbances or of the thermo-optical properties of a sample without the use of any standard, provided that all the optical and geometrical parameters of the experimental set-up are known. Time-resolved experiments have been applied for the determination of k and C_p, from the experimental values of θ and t_c, in the study of electrolyte and surfactant effects on the thermo-optical properties of water.[44] The method is also very useful when reference standards are not available, such as in the measurement of thermal diffusivities of skin[45] or of soda-lime glass.[46]

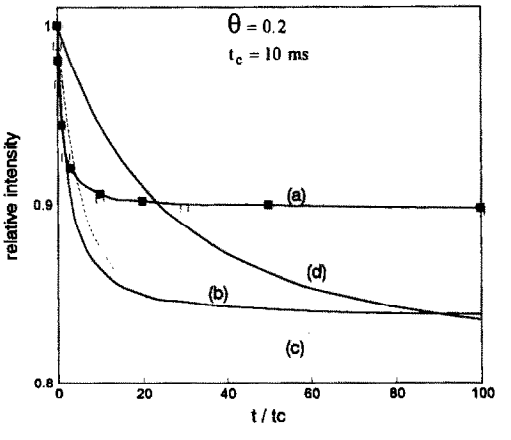

Fig. 3. Time-dependence of the thermal lens signal shown as the relative intensity *vs.* t/t_c, based on the aberrant thermal lens model, for different optical configurations of the experimental set-up: (a) single-beam, equation (39), (□), and mode-matched dual-beam, equation (41), (■) configurations; mode-mismatched dual-beam configuration, equation (40), with (b) $m = 4$, (c) $m = 10$ and (d) $m = 50$.

REFERENCES

1. A. C. Tam, in *Ultrasensitive Laser Spectroscopy*, D. S. Kliger (ed.), Chap. 1. Academic Press, New York, 1983.
2. C. K. N. Patel and A. C. Tam, *Rev. Mod. Phys.*, 1981, **53**, 517.
3. A. C. Tam, *Rev. Mod. Phys.*, 1986, **58**, 381.
4. N. J. Dovichi, *CRC Crit. Rev. Anal. Chem.*, 1987, **17**, 357.
5. S. E. Bialkowski, *Spectroscopy*, 1986 **1**, 26.
6. M. D. Morris and K. Peck, *Anal. Chem.*, 1986, **58**, 811A.
7. N. J. Dovichi, *Prog. Anal. Spectrosc.*, 1988, **11**, 179.
8. A. Berthod, *Spectrochim. Acta Rev.*, 1990, **13**, 11.
9. A. Lachaine, R. Pottier and D. A. Russell, *Spectrochim. Acta Rev.*, 1993, **15**, 125.
10. S. E. Braslavsky and G. E. Heibel, *Chem. Rev.*, 1992, **92**, 1381.
11. J. Georges, *Spectrochim. Acta Rev.*, 1993, **15**, 39.
12. H. L. Fang and R. L. Swofford, in *Ultrasensitive Laser Spectroscopy*, D. S. Kliger (ed.), Chap. 3. Academic Press, New York, 1983.
13. J. M. Harris, in *Analytical Applications of Lasers*, E. H. Piepmeir (ed.), p. 451. Wiley-Interscience, New York, 1986.
14. J. M. Harris and N. J. Dovichi, *Anal. Chem.*, 1980, **52**, 695A.
15. J. Georges and J.-M. Mermet, *Analusis*, 1988, **16**, 203.
16. G. C. Wetsel and S. A. Stotts, *Appl. Phys. Lett.*, 1983 **42**, 931.
17. W. B. Jackson, N. M. Amer, A. C. Boccara and D. Fournier, *Appl. Opt.*, 1981, **20**, 1333.
18. A. C. Boccara, D. Fournier and J. Badoz, *Appl. Phys. Lett.*, 1980, **36**, 130.
19. P. E. Poston and J. M. Harris, *J. Am. Chem. Soc.*, 1990, **112**, 644.
20. M. J. Pelletier, H. R. Thorshein and J. M. Harris, *Anal. Chem.*, 1982, **54**, 239.
21. N. J. Dovichi, T. G. Nolan and W. A. Weimer, *Anal. Chem.*, 1984, **56**, 1700.
22. T. G. Nolan, W. A. Weimer and N. J. Dovichi, *Anal. Chem.*, 1984, **56**, 1704.
23. J. P. Gordon, R. C. C. Leite, R. S. Moore, S. P. S. Porto and J. R. Whinnery, *J. Appl. Phys.*, 1965, **36**, 3.
24. R. C. C. Leite, R. S. Moore and J. R. Whinnery, *Appl. Phys. Lett.*, 1964, **5**, 141.
25. K. Miyaishi, T. Imasaka and N. Ishibashi, *Anal. Chem.*, 1982, **54**, 2039.
26. S. Wu and N. J. Dovichi, *J. Appl. Phys.*, 1990, **67**, 1170.
27. K. L. Jansen and J. M. Harris, *Anal. Chem.*, 1985, **57**, 1698.
28. J. F. Power and E. D. Salin, *Anal. Chem.*, 1988, **60**, 838.
29. J. F. Power, *Appl. Opt.*, 1990, **29**, 52.
30. C. Hu and J. R. Whinnery, *Appl. Opt.*, 1973, **12**, 72.
31. J. Stone, *J. Opt. Soc. Am.* 1972, **62**, 327.
32. J. R. Whinnery, *Acc. Chem. Res.* 1974, **7**, 227.
33. K. J. Skogerboe and E. S. Yeung, *Anal. Chem.*, 1986, **58**, 1014.
34. S. J. Sheldon, L. V. Knight and J. M. Thorne, *Appl. Opt.*, 1982, **21**, 1663.
35. C. A. Carter and J. M. Harris, *Appl. Opt.*, 1984, **23**, 476.
36. R. L. Swofford, M. E. Long and A. C. Albrecht, *J. Chem. Phys.*, 1976, **65**, 179.
37. C. A. Carter and J. M. Harris, *Anal. Chem.*, 1983, **55**, 1256.
38. H. L. Fang and R. L. Swofford, *J. Appl. Phys.*, 1979, **50**, 6609.
39. T. Berthoud, N. Delorme and P. Mauchien, *Anal. Chem.*, 1985, **57**, 1216.
40. J. Shen, R. D. Lowe and R. D. Snook, *Chem. Phys.*, 1992, **165**, 385.
41. W. A. Weimer and N. J. Dovichi, *Anal. Chem.*, 1985, **57**, 2436.
42. M. C. Gupta, S. D. Hong, A. Gupta and J. Moacanin, *Appl. Phys. Lett.*, 1980, **37**, 505.
43. N. J. Dovichi and J. M. Harris, *Anal. Chem.*, 1981, **53**, 106.
44. M. Franko and C. D. Tran, *J. Phys. Chem.*, 1991, **95**, 6688.
45. S. M. Brown, M. L. Baesso, J. Shen and R. D. Snook, *Anal. Chim. Acta*, 1993, **282**, 711.
46. M. L. Baesso, J. Shen and R. D. Snook, *Chem. Phys. Lett.*, 1992, **197**, 255.